The Barbados Cloud Observatory

Anchoring Investigations of Clouds and Circulation on the Edge of the ITCZ

Bjorn Stevens *

Max-Planck-Institut für Meteorologie, Hamburg Germany

David Farrell

Caribbean Institute for Meteorology and Hydrology, Bridgetown, Barbados

Lutz Hirsch, Friedhelm Jansen, Louise Nuijens, Ilya Serikov, Björn Brügmann

Max-Planck-Institut für Meteorologie, Hamburg, Germany

Marvin Forde

Caribbean Institute for Meteorology and Hydrology, Bridgetown, Barbados

Holger Linne, Katrin Lonitz

Max-Planck-Institut für Meteorologie, Hamburg, Germany

Joseph M. Prospero

Rosenstiel School of Marine and Atmospheric Science, University of Miami, USA

**Corresponding author address:* Bjorn Stevens, Max-Planck-Institut für Meteorologie, Bundesstrasse 53, 20146 Hamburg, Germany

E-mail: bjorn.stevens@mpimet.mpg.de

ABSTRACT

Clouds over the ocean, particularly throughout the tropics, are poorly understood and drive much of the uncertainty in model based projections of climate change. In early 2010 the Max Planck Institute for Meteorology and the Caribbean Institute for Meteorology and Hydrology established a cloud observatory on the windward edge of Barbados. At 13 °N the observatory samples the seasonal migration of the inter-tropical convergence zone (ITCZ), from the well-developed winter trades dominated by shallow cumulus, to the transition to deep convection as the ITCZ migrates northward during boreal summer. The unique setting of the Barbados Cloud Observatory allows for tracking the influence of Saharan dust and biomass burning over South America and Africa. In its five years of operation, and through complementary intensive observing periods using the German High Altitude Research Aircraft, HALO, the observatory has become a cornerstone of efforts to understand the relationship between cloudiness, circulation and climate change.

Clouds are at the heart of some of the most fascinating questions posed by climate change. As highlighted by **?**, the coupling between clouds and circulation systems influences not just the pace of warming but also the pattern of the general circulation response to this warming. Cumulus clouds confined to the lower troposphere, like those that prevail in the trades, have long been appreciated as central to the question as to how much surface temperatures will rise with increasing concentrations of carbon dioxide in the atmosphere (**??**). But specific hypotheses for how clouds change with warming have only recently begun to be developed, mostly to suggest that these clouds will change in a way that amplifies warming (**??**). Deep and high clouds profoundly affect the atmospheric circulation and how it may change with warming (**?**) and their changes may also influence the pace of warming. If (as some studies suggest) deep convective clouds aggregate more strongly with increasing temperatures, Earth's atmosphere may become more efficient in radiating heat to space as it warms. This would reduce the warming associated with a given increase in the concentration of atmospheric carbon dioxide (**???**). But here again low clouds may play a decisive role, both because the processes leading to convective aggregation are rooted in shallow marine boundary layers like one finds in the trades (**?**), and because the fate of low clouds becomes more important to understand if high clouds retreat with warming. Understanding climate change is thus synonymous with understanding patterns of cloudiness; and although Earth's atmosphere supports many different cloud regimes, advancing understanding of those in the trade wind regions has the potential to advance the science on many fronts.

The way in which a poor understanding of low clouds translates into uncertainty in the response of the climate system to forcing can be illustrated by a simple example. Through the course of development of the new version of the Max Planck Institute for Meteorology Earth System Model, the MPI-ESM, particular attention was devoted to fixing errors that had been identified in an earlier version of that model (**?**). The initial result of this process was a model that had an abundance of low clouds, concentrated near cloud base, in the trades, and over the oceans more generally. Because the cloudiness in this layer proved to be very sensitive to the surface temperature (Fig. 1) this version of the model had an exceptionally strong response to forcing. But cloudiness in this layer also proved to be rather sensitive to parameter settings which controlled the lateral mixing rate of shallow cumulus. For a different choice of parameters the cloud-base peak in cloud amount is much less pronounced, changes less with warming, and the climate sensitivity of the model is more than halved (Fig. 1). This simple example is consistent with analyses of other models (**??**), and explains why a better understanding of trade-wind clouds is very much at the center of efforts to better understand the expected pace of warming.

Understanding cloudiness in the trades is also important for a more general comprehension of Earth's general circulation. As long as Earth has had an atmosphere and an ocean, it probably has had trade winds, and in these trade winds different types of clouds. Heating in the equatorial regions draws low-level flow equator-ward and, because of angular momentum conservation, westward. As these easterlies pass over a progressively warmer ocean, convective turbulence mixes moisture away from the surface. This creates and sustains a relatively shallow and moist marine layer despite the drying from large-scale subsidence. A temperature inversion often caps this marine layer, and limits cumulus development, so that stratiform clouds originating from the outflow of underlying cumulus (stratocumulus cumulogenitus) is not uncommon. In yet more suppressed conditions a tenuous layer of cumulus (humulis) may still be evident. In response to slight disturbance, deeper cumulus (congestus), reaching to (and even above) the freezing level, may be a source of heavy, albeit brief, showers. The trades, imbued with the properties of the upper ocean, most of the time define a somewhat shallower (1-3 km) cooler and moister layer sustained by ordinary cumulus. Though prevalence remains an appropriate adjective for the trades, these examples emphasize that subtle meteorological variations are marked by variability in cloudiness (e.g., **??**) and the vertical distribution of moisture. These variations influence the radiative cooling of the atmosphere and in so doing help determine the structure of much larger-scale circulations (**???**).

Remarkably, there exists a paucity of measurements tailored to an understanding of processes that control the structure of the trade-wind layer and the patterns of cloudiness therein. Major measurement initiatives are frequent in regions of stratocumulus (e.g. **?????**) as are field programs in regions of deeper convection (e.g., **????**). In both cases, regimes of more broken, trade-wind-like clouds may be sampled serendipitously, but are not generally the focus of measurements. RICO, the Rain In Cumulus Over the Ocean field study (**?**) is the exception that proves the rule. As even for RICO, which combined measurements from three airborne platforms with ship and ground based remote sensing, the focus was more on microphysical processes that influence rain formation in shallow clouds, rather than on the interplay of cloudiness with its large-scale environment. There have been many other field studies focused on rain forming processes in trade-wind convection (e.g., **???**). The last field studies to attempt to understand larger-scale cloud controlling factors in the trades, i.e., the Barbados Oceanographic and Meteorological Experiment, (BOMEX, **?**) and the Atlantic Tradewinds Experiment, (ATEX, **?**), were nearly fifty years ago. These seminal studies, both of which took place in 1969, still constitute the benchmark for simulations of cloudiness in the trades (**??**).

This absence of empiricism has only been tolerable because of a growing record of satellite measurements (e.g., **????**). Although helpful, especially measurements from active sensors, satellites have several disadvantages for studies of clouds in the trades: trade-wind clouds comprise many smaller clouds that are poorly sampled by satellites; the presence of upper level clouds, whether it be overlying cirrus or stratocumulus-cumulogenitus near the trade-inversion, obscures a view of processes near cloud base; the highest resolution sensors poorly sample evolution in time; and finally, the use of satellite measurements to advance process understanding is often dependent on meteorological reanalyses, which in the lower tropical-troposphere are less constrained by data.

To fill this gap in the empiricism and thereby advance understanding of the Tradewinds and their clouds, we have established a cloud observatory on the island of Barbados (13 °N, 59 °W) . Our observatory, the Barbados Cloud Observatory (BCO), was constructed very much in the spirit of long-term European ground based observatories that form the basis of CloudNet (**?**), and the US Department of Energy's Atmospheric Measurement Program (ARM) Climate Research Facilities (**?**). These other observatories are all situated in the extra-tropics. With the closing of the tropical ARM sites, the BCO stands out as the only advanced, long-term, ground based measurement station in the broader maritime tropics. As such, in addition to informing understanding of factors controlling clouds in the tropics in its own right, the BCO is increasingly being used as an anchor for small field studies,

Having sketched out the motivation for a cloud observatory in the trades, in the following pages we explain why we chose Barbados as the location for our observatory, the general meteorological conditions at the observatory, and the evolving measurement infrastructure at the BCO. A few of the insights that have been gleaned from the first five years of operations are also presented. It is hoped that this information proves useful for those interested in using the data we collect at the BCO, or in collaborating on the design of future field studies anchored by the BCO. Further, more technical, information about the measurement systems and their evolution is provided in the form of an electronic summary. The data is freely available to the community and can be accessed by contacting the authors.

Why Barbados?

Barbados offers many attractive features for a ground-based cloud observatory in the tropics. Foremost is its location, on the edge of the Atlantic Intertropical Convergence Zone (ITCZ), where it samples steady trade-wind conditions for about half the year. Although often thought of as a Caribbean Island, Barbados sits firmly in the Atlantic ocean, some 150 km east of the Windward Islands that form the eastern border of the Caribbean sea. Unlike the Windward Islands, which are volcanic in origin and whose peaks (reaching nearly 1500 m) interact strongly with the impinging trades (**?**), Barbados is relatively flat (Fig. 2), and consists of a foundation of limestone and accumulated sediment. Geologically it was formed through a succession of coral plateaus (still evident in maps of its relief) that have risen out of the water as a result of the gradual, but episodic tectonic uplift associated with the collision of the Caribbean and Atlantic plates. This uplift forms the geological connection between the Windward Islands and Barbados. This also means that windward of Barbados the nearest land is the Cape Verde Islands nearly 3700 km away. Dakar, on the western-most point of the African mainland, is more than 4500 km away.

Barbados is also logistically attractive. A well maintained network of roads, and access to internet and power across the island greatly facilitates the maintenance of advanced remote sensing instrumentation. An international airport (Grantley Adams) provides daily connections to major international hubs, and a deep water harbor (the Port of Bridgetown) facilitates the transport of large equipment by ship. In addition, Barbados hosts the University of the West Indies, Cave Hill campus and the Caribbean Institute for Meteorology and Hydrology (CIMH). Together they provide access to students, technical expertise and an understanding of the local meteorology. The CIMH supports the maintenance of a network of measurement stations, including a modern Gematronik S-band polarimetric radar that has been in operation since 2008, and has a long history of cooperation with the University of Miami in the establishment and maintenance of mineral dust measurements.

Although Barbados is a relatively well populated island, most of the development is on its south-western (downwind) side. Eighty percent of its 280 000 inhabitants concentrate in the five parishes in and around the lowlands surrounding the capitol of Bridgetown. As a result the upwind side of the island, where the BCO is situated, remains relatively wild and undisturbed.

Meteorological Conditions Sampled by the Observatory

Barbados is on the edge of the ITCZ only in an annually averaged sense. During the dry season in boreal winter, the ITCZ stretches along a line near, or just north of, the equator over the Atlantic, spreading south of the equator over the South American and African continents (**?**). During this period the predominant flow is from the east-northeast. In Boreal summer the ITCZ migrates poleward, extending northwestward, from the central Atlantic toward Barbados (Fig. 3). During this period winds out of the east are more common although for episodes of active deep convection, the onshore flow may even have a southerly component. These seasonal swings subject Barbados to a wide variety of tropical circulation systems, including the odd Hurricane – Tomas formed over the BCO in 2009. Seasonal shifts in the wind also modulate aerosol transport, including that from biomass burning, and mineral dust raised from Africa (e.g., Fig. 4), helping to create a laboratory for understanding aerosol-cloud and aerosol-radiation interactions.

An analysis of two years of daily ten-day back trajectories, initiated over Barbados at a height of 3 km above sea level, indicates that in the dry season (December-May) roughly half of the air masses originate east of 55 °W and north of 10 °N. This fraction increases to nearly two thirds in the wet season (June-November). Of these back trajectories, most (55%) pass over the European or African continents during the wet-season but relatively few (8 %) during the dry season.

In both seasons streamlines of the low-level (10 m) flow connect Barbados to a second measurement station on the Azores, well upstream of Barbados (Fig. 3). The Graciosa station (operated temporarily during 2009 and 2010 **??**) began operations as a permanent station in September of 2013.

Barbados well samples the circulation characteristics of the broader tropical oceans. Subsidence prevails during the dry winter months from December to June, and low-level convergence supports convection in a wet season that peaks in October, but lasts from June through December (Fig. 5). In the annual mean, the distribution of the vertical at 500 hPa motion mirrors that of the broader tropics (Fig. 6); so despite its pronounced seasonal cycle, the mean vertical motion nearly vanishes (-2 hPa). Tropical sites that have been maintained in the past, most prominently on the island of Nauru in the Pacific. There the annually averaged vertical velocity is nearly an order of magnitude larger (-16 hPa) than over Barbados, which biases its climatology more toward the wet tropics. During the rainy season, less precipitation forms over Barbados, as compared to other regions in the tropics with the same amount of vertical motion. This is indicative of greater ventilation by the low entropy air of the subtropics even when deep convection prevails; in the middle of its wet season, Barbados still feels the influence of the trades.

During boreal summer, the swing of precipitation away from the southern hemisphere (over land) and a more easterly orientation of the low-level flow, is accompanied by significant dust transport from the Sahara. Dust transport over Barbados maximizes in June and July (**??**) during which time a Saharan Air Layer is frequently observed above the trade inversion in the layer of easterlies between 1.5 and 4.0 km (**?**). An example of such a layer is shown in Fig. 4. The peak in the dust layer above the trade-inversion likely reflects the efficiency of wet scavenging and removal of dust below the inversion, where shallow cumulus are prevalent and frequently precipitate. Dust transport from Africa has long motivated measurements on Barbados (**?**), as its prevalence was noted in early field studies such as BOMEX (**?**), which motivated a program of continuous dust and aerosol measurements that continues to this day (**?**). Studies have shown that it takes about a week for the dust to be transported from its source regions in Africa, and that the summertime dust transport is modulated by easterly waves, with ten-fold or larger daily variations in the amount of dust. Aged dust is known to be an effective cloud condensation nuclei (CCN). Hence the sedimentation of dust and its downward mixing through entrainment provide a source of CCN to the boundary layer (**?**). The area near and upstream of Barbados thus provides a natural laboratory for exploring the sensitivity of shallow cumulus to large changes in the number of available CCN (**?**).

The Barbados Cloud Observatory, BCO

The BCO is situated at Deebles Point, a relatively remote promontory on the upwind (eastern) shore of the island, Fig. 2. The BCO instrumentation is set back from the shore by about 30 m and the 17 m elevation of the site keeps it above the wave break. Ragged Point, the site of long-term aerosol and trace gas measurements lays across a small cove, 400 m to the northwest. At Ragged point, in addition to aerosol measurements by the University of Miami group, an AERONET station has been in operation since 2007, and one of only two Advanced Global Atmospheric Gases Experiment (AGAGE) stations in the tropics since 1978 (**?**).

The measurements at the BCO are centered around active radar and lidar profiling of precipitation, clouds, water vapor and aerosol. An overview of the BCO instrumentation is provided in Table 1, technical and operational details about the site are available in the electronic supplement. The lidar and cloud radar are among the most advanced instruments of their kind world-wide, and have formed the core for a broader and expanding suite of instruments that have been maintained since operations began on 1, April 2010. These instruments, which are described more fully in the electronic supplement to this manuscript, include a second scanning cloud radar, a water-vapor DIAL lidar and a microwave radiometer for atmospheric profiling (?) which have been deployed at various times over the first five years of BCO operations. Beginning in March 2015 instrumentation has been added for measuring broadband visible and infrared irradiances. In the summer of 2015, the scanning cloud radar will be replaced with a newer system that has a much larger (2m) dish, greater sensitivity, and is set inside a clutter fence to remove signals from side-lobes. A wind lidar will also be installed. A new high-power Raman lidar system is under development and will be installed at the BCO in the summer of 2016. The new system has the ability to measure daytime water vapor and its high-power will facilitate much higher frequency humidity profiling. Its measurements, on the scale of meters, will thus resolve the humidity structure at the very edge of a cloud and help inform understanding of cloud mixing processes.

Water vapor, aerosols, clouds and precipitation at the BCO

Because climate-change cannot be observed before it happens, the ability to anticipate changes depends on the extent to which insight into processes relevant for climate change can be inferred from present and past fluctuations of the system. Below we give a glimpse of some of what has been learned over the first five years of measurements also to guide the possible use of our data by others.

The seasonal migration of the ITCZ and accompanying circulation shifts are associated with large changes in cloudiness. This is evident when comparing measurements in February and October as compiled during the first two years of operations at the BCO. During October (taken to be representative of the wet season) mid-level and high cloudiness (above 3 km) is pronounced. The contribution of high-clouds (above 9 km) to the cumulative cloud cover above is nearly five times larger during October than it is in February (Fig. 7). Because cloudiness in the lower troposphere changes much less across the seasons, cloud cover is greatest overall during the wet season; radar derived cloud-cover is 0.5, compared to 0.36 during the dry season (Fig. 7b). But one doesn't need a ground based observatory to know that the wet season is cloudier over Barbados.

What is surprising, and what could not have been readily deduced from satellites, is that the contribution of clouds below 1 km to cloud cover doesn't vary with season. Cloud cover from low clouds in February is indistinguishable (0.22, dotted line) from that which is measured in October, or any other month for that matter. This finding has obvious implications for the questions raised by Fig. 1. Differences begin to become evident when including cloudy points that first occur between 1-5 km (dashed line). Cloud cover increases only slightly to 0.26 in the wet season, and substantially to 0.34 in the dry season when contributions in this layer are considered. Although the wet season has more high cloud that contributes to cloud cover, in the dry season this is offset by the additional cloud between 1-5 km. Relatively more cloudiness in the layer between 1.5 km and 3 km over the BCO has been shown by **?** to be associated with more stratiform clouds, associated with low-level cumulus clouds detraining at or into the trade-inversion – stratocumulus cumulogenitus. On monthly timescales low-cloud amount correlates most strongly with wind speed, which is higher in the dry season. Enhanced stability in the lower troposphere during the dry season also appears to play a role in the enhanced low-level cloudiness (**?**).

Cloudiness appears more bimodal than trimodal over Barbados, although a very faint hint of a tertiary maximum in cloudiness at 6.5 km is evident over the BCO during the dry season, and thereby reminiscent of the trimodal distribution of clouds observed by **?** in the tropical west Pacific. Even if significant this third maximum appears somewhat higher than the average melting-level cloudiness that **?** focused on. Analysis of the radar data show this peak in cloudiness to be associated with isolated cumulus congestus systems. Such a feature is not evident in the wet-season, although mid-level cloudiness is on average higher as compared to the dry season and the atmosphere overall much more humid through a deeper layer. During February the mean humidity between 4 km and 9 km is near 10 %; in the wet season it is closer to 50 %. Differences between the wet and dry season humidity are strikingly similar to differences between the dry and precipitating regions in simulations of radiative convective equilibrium (e.g., Fig. 4 in **?**), suggesting that these rather idealized simulations might capture some of the effects associated here with much larger-scale circulations.

These seasonal shifts in cloudiness at the BCO are proving helpful as a baseline for evaluating the representation of trade-wind cloudiness in large-scale models (**?**). Although it is not obvious that measurements at a point in the trades can constrain the representation of clouds in the trades more broadly, an analysis of both models and data suggest that constraints on cloudiness from the BCO can indeed inform the representation of trade-wind clouds in models (**??**). Measurements at the BCO thus provide the basis for the suggestion that large-scale models with parameterized shallow convection do an adequate job of representing the basic depth and structure of the cloud layer, but that cloudiness near cloud base is more constant in the data then it is in models, and that cloudiness varies with wind-speed in ways that models struggle to capture (**??**).

The BCO also functions as a laboratory for studying aerosol-cloud interactions. Aerosol optical depth can vary greatly, largely as a result of dust transport from North Africa. Dust episodes can produce daily averaged optical depths larger than 0.4, and are most common in the May-September time-frame, although dust events do occur in some years already in early spring, Fig. 8. During the dry season, particularly January and February, the flow from the east-northeast is less aerosol laden, with optical depths remaining well below 0.05 for extended periods of time, and very little dust is evident. The interplay between dust transport and precipitation leads to much more variance in aerosol optical depth during the wet season, with aerosol optical depths dropping to values less than 0.01 and reduced amounts of sea-salt. Such very clean periods occur more often during the wet season when wet scavenging is strong, but also because climatologically lighter winds lead to less sea-salt aerosol to begin with (Fig. 8b). The slightly higher clear sky extinction (Fig. 7d) above 5 km in February, is consistent with slightly more dust during this period, although differences between dust amounts in February and October are small (Fig. 8b).

Although the aerosol varies considerably over the BCO, seemingly much more profoundly than the meteorology, we have been surprised at how difficult it is to demonstrate a robust influence of the aerosol on important cloud properties, such as the tendency to form precipitation. An analysis of two years of data from the KATRIN cloud radar shows a profound influence of slight changes in ambient relative humidity on cloud development, but no robust signature of aerosol effects (**?**). This result stands in marked contrast to the representation of such effects in many global models and inferences from satellites, wherein for the latter it is not possible to control for small variations in important factors like the relative humidity of the cloud layer.

Anchoring investigations on the edge of the ITCZ

Measurements at the BCO are increasingly acting as an anchor for field campaigns by groups from around the world: The Barbados Aerosol Cloud Experiment BACEX in 2010, and two CARRIBA Campaigns (Cloud, Aerosol, Radiation and tuRbulence in the trade wInd regime over BArbados) in November 2010 and April 2011 (**?**). During CARRIBA a suite of in situ particle measurements were made at the neighboring Ragged Point, and profiling of the turbulent structure of the cloudy boundary layer upwind of the BCO was performed with a helicopter borne payload. During the recent SALTRACE 2013 campaign additional lidars and in situ particle samplers were deployed both on the CIMH campus and at Ragged Point, and air masses were sampled from the DLR Falcon aircraft, which in addition to an array of particle probes also deployed a wind lidar system.

The BCO is also anchoring studies of tropical and trade wind convection performed with the help of the German High Altitude and Long-range research aircraft – HALO (Box 1). The first HALO campaign, NARVAL, took place between 10-20 December 2013 (**?**, see also the electronic supplement). NARVAL comprised eight flights over the tropical North Atlantic (Fig. 11) designed to test its payload of nadir looking remote-sensing instruments, and investigate the extent to which measurements at the BCO were representative of the broader trades. Seven missions included long coincident legs along the path of the A-Train constellation of satellites. The legs allowed for a comparison of the lidar and radar remote sensing from HALO to be compared with the CALIOP lidar on CALIPSO and the Cloud Profiling Radar on CloudSat. Sixty-seven dropsondes were also successfully launched from HALO, most in a region of the sub-tropical Atlantic (Fig. 11).

Conditions during NARVAL where characterized by a relatively homogeneous large-scale environment, and an exceptionally dry free-troposphere, very much consistent with the measurements at the BCO. Over a stretch of thousands of kilometers convection was confined to a shallow (1.5 km to 3 km) marine layer, above which the atmosphere was very dry and cloud free. The homogeneity in the large-scale conditions meant that a clear trade-wind structure, with a pronounced trade-wind temperature inversion and hydro-lapse, also emerges from the mean sounding (Fig. 9) taken from the forty-six sondes launched south of 20 °N and west of 25 °W. The main features of this mean sounding are also evident in individual soundings. Here the top of a relatively thick inversion layer is defined by the maximum in the saturated moist static energy, and the minimum in moist static energy at about 3 km. It demarcates the depth of the deepest convective clouds. For the most part, moist convection is confined between the top of the sub-cloud layer at about 600 m and the base of the trade-wind inversion at about 1.75 km, and the free tropospheric humidity is at most a few percent (FIg. 9), similar to what is observed in the winter trades at the BCO.

During the period of the NARVAL flights, the BCO was influenced by deeper convection that was prevalent south of the area of flight operations, near the Guyana coast . This is evident in lower values of outgoing long-wave radiation in Fig. 11, which extended northward toward Barbados on some of the days, e.g., December 14th. The radar imagery from BCO cloud radar KATRIN shows the contrast between periods of deeper convection and the more suppressed conditions more typical of the trades (Fig. 10), and what was sampled by HALO. Deeper convection over and south of Barbados maintained elevated cirrus outflow layers on 14 December, transitioning to more suppressed conditions with diminishing high clouds and convection capped at about 2-3 km thereafter. The three modes of convection seen in this three day period are similar to what is seen in the average over four years (Fig. 7).

The radar imagery emphasizes that very shallow moist convective systems are not infrequent, and can be intense. This is the case for an event measured around 13:30 UTC on 15 December (Fig. 10), for which a convective cluster with tops only at 2.5 km sustains an echo that is greater than 40 dBZ. These types of system are commonplace in the BCO record, as evidenced by the daily quicklook imagery. Similar systems featured prominently in the distribution of cloudiness over the broader Atlantic trades during the HALO overpasses (see electronic supplement), and were also often observed during RICO (**?**). This suggests that the convective systems sampled by the BCO are not just a local feature but play an important role in the mass and moisture budgets in the trades, and as such are important for interpreting signatures of precipitation by satellite (**?**).

In demonstrating the capability of the HALO aircraft to characterize the large-scale environment through active remote sensing and from dropsondes, NARVAL has set the stage for subsequent field studies. For instance, NARVAL-II, will take place in August of 2016 and will use Barbados as its base of operations. During NARVAL-II HALO will explore the capability of measurements of the divergence of the horizontal wind (from dropsondes) and thermodynamic profiles (also from remote sensing) to constrain the mass, heat and moisture budgets in an area of some $10^4\,\mathrm{km}^2$, typical of the grid-cell in a general circulation model. These types of measurements are being performed to help understand the interaction of shallow convection with its large-scale environment, including the role of shallow trade-wind layers in the organization of deeper convection nearby. NARVAL-II will also help inform the design of, and contribute to, a larger, multi-platform field study, being proposed for 2019. This campaign, (Elucidating the Role of Cloud-Circulation Coupling in Climate, EUREC^{4}A) is a French initiative to leverage ongoing measurements by HALO, and at the BCO, to explore new ideas for testing our understanding of how clouds and convection interact with the large scale environment. To the extent that measurements during EUREC^{4}A and the long-term context of the BCO gives impetus to further international contributions, a deeper understanding of cloudiness within the trades seems by no means out of reach.

Box 1: HALO

HALO is a Gulfstream 550 with a large-payload (2800 kg, 800 kg with maximum fuel), long range 12 500 km and a high (15.5 km) ceiling. In support of measurements at the BCO a suite of remote sensing instrumentation has been developed for HALO in cooperation with the German national aeronautics and space research center (DLR), the University of Hamburg and the University of Cologne. The instrumentation includes three banks of radiometers with 26 channels spanning the K and V bands, a K_α cloud radar very similar to the KATRIN system on Barbados, but with a somewhat reduced (-38 dBZ at 5 km) sensitivity and a water-vapor DIAL lidar (WALES). The microwave instrumentation is described in more detail by **?**. The remote sensing instrumentation looks in the nadir direction from a special belly-pod mounted on the forward fuselage of HALO (Fig. B1). Dropsondes can be launched from the rear of the aircraft, and Differential Optical Absorption Spectroscopy provide further information about the state of the airmass below HALO.

A high-resolution spectro-radiometer (HALO-SR) measured radiances in the spectral range from 0.35 to 2.0 μm, with a spectral resolution of 0.003 μm below 1 μm and 0.016 μm between 1 and 2 μm. The composition of various trace gases was measured using a Differential Optical Absorption System (miniDOAS). The HALO mini-DOAS instrument was developed by the Institut für Umweltphysik at the University of Heidelberg. It consists of a six channel (UV/Vis/IR) Spectroradiometer that measures trace-gas amounts using scattered sunlight in the limb and nadir directions.

Acknowledgment. The Barbados Museum and Historical Society, which owns the land on which the BCO is situated, is thanked for making the site available for these measurements. We thank the Max Planck Society for the Advancement of Science. Tropical Rainfall Measuring Mission (TRMM) data provided by the TRMM science team through an international project jointly sponsored by the Japan National Space Development Agency (NASDA) and the US National Aeronautics and Space Administration (NASA) Office of Earth Sciences. The OLR data is taken from the AIRS instrument. DLR and the German research community is thanked for their support of HALO. HYSPLIT was used to calculate back trajectories. Steffan Bos is thanked for his analysis of the CloudSat overpasses during NARVAL and his drafting of Fig. ES1. Thorsten Mauritsen is thanked for his help with the experimental design and sensitivity study that produced Fig. 1. Saskia Brose helped processing the composition data from Ragged Point and Monika Pfeiffer contributed to the development of the electronics within the lidar system. The University of Miami site at Ragged Point is largely supported by the US NSF and NASA. J. M. Prospero gratefully acknowledges the Manning Estate, Barbados, for use of their land at Ragged Point and thanks Edmund Blades and Peter Sealy of Barbados for maintaining and operating the facility. Primary data and scripts used in the analysis and other supplementary information that may be useful in reproducing the authors work are archived by the Max Planck Institute for Meteorology and can be obtained by contacting publications@mpimet.mpg.de

ELECTRONIC SUPPLEMENT

Ground Based Instrumentation

The core BCO instruments consist of a multi-channel multi-wavelength Raman lidar system, a scanning K_α band cloud radar, a K band micro-rain radar, a ceilometer, an all sky imager and a standard weather sensor. These instruments are described further below.

(i) Raman Lidar The lidar uses a pulsed lidar beam and measures the elastic scattered light, the pure rotational Raman spectra (PRRS) and the rotational-vibrational Raman spectra of atmospheric molecules. Isolating individual spectral features of the atmospheric response, we apply the Raman lidar technique to characterize the scattering properties of atmospheric aerosols and to measure the air temperature and humidity. The lidar measures at nine spectral channels up to altitudes of 15 km, with a 7.5 m range gate. Three telescopes permit near-, mid- and far-field measurements. The different products that can be obtained from the lidar are particle backscatter, particle extinction, depolarization ratio, lidar ratio, water vapor mixing ratio, aerosol optical depth, and temperature. The present Raman lidar system measures water vapor mixing ratio and humidity during nighttime hours only, providing every other measurements round-the-clock during rain-free conditions. A new higher powered system, which will allow daytime humidity measurements, is being developed and is scheduled to become operational in 2016. The combination of particle backscatter measured at three wavelengths, particle extinction measured at two wavelengths, and particle depolarization ratio will also give information on the aerosol types. Particle backscatter is derived directly as the ratio of atmospheric lidar returns in the elastic and the pure rotational Raman channels. Thanks to the relatively small difference in wavelength of backscattered light for these two channels the corresponding differential atmospheric extinction is negligible. More information about the individual measurements is provided in Table ES1

(ii) Scanning Cloud Radar The radar is a scanning K_α-Band (35.5 GHz) polarized Doppler cloud radar with a high sensitivity (-52 dBZ at 5 km with 100 m range gates and 30 s averaging). At 35 GHz one expects attenuation in the presence of water vapor and condensate, but much less than at W-band. As such this frequency range strikes a good compromise between achieving the sensitivity that one desires for sensing clouds, and the range required to profile through the depth of the atmosphere. The radar was named KATRIN, for Katrin Lehmann, a brilliant young scientist who died in a hiking accident in May 2009, shortly before she was to have joined the BCO team. KATRIN's antenna can be scanned with a full 360 degree in azimuth and $\pm 90^\circ$ in elevation. The 1.2 m antenna has a beam width of 0.5 degrees. The radar reaches full sensitivity at a range of 500m, hence provides a good cloud base detection capability. The high range resolution of up to 10 m (typically 30 m) together with the narrow beam width allows for fine scale observations of the cloud structure. The Doppler velocity resolution of up to 0.05 m s^{-1} provides an insight into the turbulent fine structure of clouds. The radar receives the linear polarized signal in co- and cross polarized orientation and thus provides the Linear Depolarization Ratio (LDR) that is a very helpful information to discriminate between different target types, such as liquid from ice, or insects. The system is fully automated and remotely controlled.

For roughly the first year of operation KATRIN alternated between azimuth scans (first at four elevation angles 5°, 12°, 22° and 45°, later only at the lower two elevations), range-height indicator scans, and vertical staring. The scanning data was used to evaluate whether or not there was an apparent island effect, by comparing joint height versus reflectivity histograms at different ranges, and at different times of the day, but a significant signal was not found and thereafter (since 20.12.2011) the radar has only been operated in a vertically pointing mode. The vertically pointing mode is preferred for a number of reasons: an analysis of the scanning data showed that the radar range (which is limited to about 15 km by attenuation to about when scanning at low elevation angles) was not sufficient to measure convective life-cycles in the scanning mode, the vertical pointing mode is advantageous for microphysical retrievals, and is entails less wear and tear on the instrumentation.

(iii) Micro Rain Radar The Micro Rain Radar MRR-2 is a frequency modulated continuous wave radar operating in the K-band (24 GHz). It retrieves the drop size distributions and its moments, radar reflectivity, fall velocity of hydrometeors simultaneously on vertical profiles extending up to 3 km. As such it can sample the entire rain system from shallow convective systems whose tops are frequently below 3 km. Two MRRs are deployed on Barbados, one at the BCO and one at CIMH. Both instruments are configured to have a vertical resolution of 100 m so as to provide sufficient range coverage. Due to the high sensitivity and fine temporal resolution very small amounts of precipitation (below the threshold of conventional rain gauges) can be detected. For the chosen configuration the manufacturer specifies a detection threshold of 0.01 mm h^{-1} at 500 m for an averaging time of 10 s. The large scattering volume (compared to in situ sensors) allows to derive statistically stable drop size distributions within a few seconds. The droplet number concentration in each drop-diameter bin is derived from the backscatter intensity in each corresponding frequency bin. In this procedure an empirical relation between terminal falling velocity and drop size is exploited.

(iv) Ceilometer A Jenoptik 15k laser ceilometer with a 0.4 mrad field of view measures backscattered energy at 1064 nm wavelength. The ceilometer is designed to operate up to heights of 15 km with a resolution of 15 m and a temporal resolution of 30 s, although individual returns are increasingly difficult to distinguish from background noise with increasing altitude, limiting its effectiveness at the highest rate of sampling to the lower 4 km of the atmosphere. **?** demonstrated that the ceilometer returns are useful to derive cloud base heights (which include actual cloud base heights,

but also cloud edges) by comparing gradients in returns to a threshold based on the background noise level. During the period between Dec 6, 2011 and 9 March 2012 the 15k model has been temporarily replaced by the Jenoptik 15k-X model. The 15k-X, has a larger, 1.7 mrad, field of view and is thus subject to more background noise during daylight hours – especially at low zenith angles in the tropics.

(v) All-Sky Imager A self-made all-sky imager provides a high resolution digital photo from the sky above the site every minute. It was a project of the apprentices of the MPI-M workshop based on a prototype from John Kalisch who at the time was working at the Institute for Sea Research in Kiel, Germany. It consists of a digital Camera Canon Photoshot G9 with 12.1 Megapixel and a Fisheye objective Raynox DCR-CF185PRO build into an outdoor housing.

(vi) Meteorological Instrumentation: Continuous meteorological measurements are provided by a VAISALA WXT520 sensor which is mounted to a mast above one of the sea-tainers. The sensor provides measurements of wind speed and direction, rainfall, temperature, humidity and barometric pressure at 10 s intervals. During the field studies such as CARRIBA and NARVAL radiosondes are launched once to twice a day from the site, and are launched irregularly throughout the year for ongoing calibration of the remote sensing instrumentation.

Supplementary Instruments

Four webcams, oriented south-east, north-east, northward and westward that take visible images of the site every minute. In addition the BCO includes an array of supplementary instruments, some of which are quite sophisticated, but have been operational only temporarily. These are described below.

(vii) Water Vapor DIAL The MPI water vapor Differential Absorption Lidar (DIAL, **?**) was operated for five months during the period between November 2011 and May 2012. The DIAL transmits in the near infrared, at 820 nm, where appropriate water vapor absorption lines are located. Elastic backscatter at two wavelengths, one adjusted to the maximum absorption and another one to the wing of the absorption line, provides the information on air humidity. Working with elastic scattering makes the technique nearly insensitive to the sky background and allows daytime retrievals of humidity, which is not possible with the present Raman lidar system. The laser cavity design allows adjusting the sounding wavelengths to the different absorption lines, which are selected according to typical air humidity in the region of observations. Usability of DIAL in the vicinity of low clouds was found to be limited due to nonlinearities in the receiving chain formed by detector, amplifiers and AD converter. Different errors in signal gradients at online and offline wavelength require manual selection of trustworthy water vapor in the range of clouds. The DIAL was also of limited use for detecting humidity above the cloud layer due to insufficient backscattered energy.

According to the DIAL data the deviation of absolute humidity from the daily average value remains in the range of $\pm$ 0.3 g m^{-3}. So if a diurnal cycle is present, it is small. This gives us confidence that the night-time humidities derived from the Raman system are representative of the daily average. The development of the new, high-powered system, which is capable of day-time humidity measurements will, however, let us test this supposition.

(viii) Scanning Precipitation Radar The Barbados Meteorological Service maintains a high performance METEOR 500S Gematronik radar. The radar operates in the S-band (10 cm), is linearly (horizontal) polarized and has been operational since 2008 with data archived since 2009. The radar uses two pulse lengths, the shorter 0.82 μs pulse provides a higher range resolution of 125 m,

a sensitivity of -4.7 dBZ at 50 km and an unambiguous range of 125 km. The longer, 2 μs pulse yields a 300 m range resolution, a sensitivity of -12.5 dBZ at 50 km and an unambiguous range of 500 km. The antenna has an 8.5 m diameter, resulting in a beam width of 1°. A full 360 ° scan can be performed in 10 s. The scan strategy presently consists of five 360° azimuth scans in three minutes, repeated every 5 minutes, so that there is a two minute interval when no data is being collected. The five elevation angles used are 0.0°, 0.5°, 2.2°, 5°, and 15°. The scanning strategy has evolved over time, but a 400 km surveillance scan at a low elevation angle has been performed every 15 minutes since the beginning of operations.

(ix) Microwave Radiometer The University of Cologne has been maintaining a scanning Radiometer Physics HATPRO radiometer, SUNHAT. SUNHAT has two receivers and measures seven brightness temperatures around the water vapor line at 22.24 GHz with 3.3° to 3.7° resolution, and seven in the oxygen complex band at 60 GHz with 2.2° to 2.5° resolution. The brightness temperatures from the water vapor line are used for water vapor profiling, the oxygen band measurements for temperature profiling. Measurements around the water vapor line are used to derive integrated water vapor (IWV) and integrated liquid water (LWP) content. The Instrument scans both in elevation and in azimuth with a step in the pointing angle of 0.6° to 0.1° in each direction respectively. The SUNHAT provided data for most of 2011, it was removed for maintenance and has since been re-installed and has been operating continuously since late 2013.

(x) Composition Measurements at Ragged Point The University of Miami Rosenstiel School of Marine and Atmospheric Sciences maintains a site with two cargo-container laboratories and a 17 m tower atop a 30 m cliff on Ragged Point. Daily aerosol filter samples are collected atop the tower and dust, non-sea-salt sulfate, nitrate and sea-salt are measured. Dust burdens are highly variable, but can be as high as 200 $\mu g\, m^{-3}$ during dust events, but even during the dustiest months

concentrations are typically much lower with median values similar to sea-salt burdens, which average around 20 μg m^{-3} with only light seasonality (Fig. 8b). Burdens of nitrate and non-sea-salt sulfate are much smaller. For the ten-year period between 2000 and 2010 daily nitrate concentrations averaged 0.49 μg m^{-3} with an interquartile range between 0.30 μg m^{-3} to 0.79 μg m^{-3} Daily sulfate concentrates averaged 1.9 μg m^{-3} with an interquartile range between 1.4 μg m^{-3} to 2.5 μg m^{-3}.

NARVAL

The Next generation Aircraft Remote sensing for VALidation studies (NARVAL) field study comprised two major phases (**?**). The South Phase was flown over the tropical and subtropical Atlantic in December 2013 and a North Phase examined precipitation from post-frontal systems in the storm tracks in January 2014. The South Phase was flown in support of operations at the BCO and is briefly summarized here.

Table ES3 lists important information from the eight NARVAL South Phase flights. Four of these flights crossed the Atlantic, the remainder took off and landed at Grantley Adams Airport. Three research flights (RF03-RF05) flew from Grantley Adams to the mid-Atlantic and returned along the same path, deviating only to fly a leg under the track of the A-train at the time of its overpass. One research flight (RF02) flew a mattress-spring pattern east of Barbados overlying an area of deep convection in the southern part of flight operations. One of the trans-Atlantic legs (RF07) included thirty-seven minutes of coordinated operations (1100-1137 UTC) with the French Falcon F20 sampling a convective system between Lyons and Tarbes. The Falcon operated its RASTA system which includes a W-band cloud radar and flew 2 km below HALO at a flight level near 10 km

Legs coinciding with an A-train overpass varied in duration from 784 s for RF01, to 1507 s for RF06, corresponding to a leg length of 188 km to 414 km. Clouds were fortuitously sampled on all A-train overpass legs. An example is shown in Fig. ES1 which also shows that CloudSat provides a very good representation of the shallow convective systems observed over the central Atlantic, only missing features in the lowest 1 km of the atmosphere. When the HAMP measurements are degraded to the resolution of CloudSat the match is even better. There is some indication that the W-band cloud radar aboard CloudSat is somewhat more sensitive to low clouds then is the K_α band radar flown as part of HAMP. There is, however, also the indication that CloudSat misses some of the intense ($>$ 35 dBZ) but narrow precipitation features (e.g., the region of very strong returns in Fig. ES1.

LIST OF TABLES

TABLE 1. Summary of BCO measurement systems. Further information about the operation and technical specifications of the measurement systems are provided in the electronic supplement.

System	Measurements
Raman Lidar	Measures particle backscatter at 355, 532 and 1064 nm. Particle extinction is derived from pure rotational Raman signals at 355 and 532 nm. The depolarization ratio is measured at 532 nm. Water vapor mixing ratio derived and air temperature from Raman signals at 355 nm. In July 2016 the existing system will be replaced by the CORAL system designed to measure humidity within 2% at a 3 m range and 5 s temporal resolution
Katrin Cloud Radar	A Metek Scanning K_α (35.5 GHz) polarized Doppler radar measures clouds and precipitation. It is operated a high (-52 dBZ at 5 km) sensitivity, and has a 0.5 ° beam width (at half maximum). In July 2015 the KATRIN system will be replaced by the new CORAL radar, which is non scanning, but has an improved (-60 dBZ at 2 km for 15 m range gates and 2 s averaging) sensitivity and a narrower (0.3 °) more isolated beam to avoid clutter.
Scanning Precipitation Radar	A high performance METEOR 500S Gematronik radar operating in the S-band measures precipitation with a 300 m range resolution and a sensitivity of -12.5 dBZ at 50 km. It has been operational since 2008 and is maintained by the Barbados Meteorological Service.
Microwave Radiometer	A scanning Radiometer Physics HATPRO Radiometer maintained by the University of Cologne measures seven brightness temperatures around the water vapor line at 22.24 GHz.
Micro Rain Radar	A frequency modulated continuous wave radar, the MRR-2, operating in the X-band (24 Ghz). Two MRRs are deployed, one at the BCO and another at the CIMH.
Ceilometer	A Jenoptik 15 K laser ceilometer with a 0.4 mad field of view measures backscattered energy at 1064 nm.
Radiation	A Solys2 sun tracker with two CP21 Pyranometers (shaded and non shaded) measuring visible radiation (0.285 - 2.80 μm), a CGR4 shaded Pyrgeometer measuring thermal radiation(4.50 - 42.0 μm) and a CHP1 Pyreheliometer for measuring direct irradiance (0.20 - 4.00 μ m). Operational since March 2015.
Wind Lidar	A Halo Photonics Stream-Line Pro wind-lidar system for profiling the wind in the lower atmosphere. To be deployed in July 2015.
Atmospheric Composition	The University of Miami makes daily filter samples from a 17 m tower (atop a 30 m cliff) at nearby Ragged Point
Standard Meteorology	Continuous meteorological measurements are provided by a Vaisala WXT520 sensor, which measures barometric pressure, humidity, precipitation, temperature, and wind speed and direction from a mast at a height of 5 m
All-sky imager	A self-made all-sky imager provides high resolution digital photograms every minute.
Web Cams	Four webcams oriented south-east, north-east, northward and westward take visible images every minute.
Water Vapor DIAL	The Max Planck Institute water vapor differential absorption lidar (DIAL, **?**) was operated for five months during the period between November 2011 and May 2012. The DIAL transmits in the near infrared, at 820 nm, where appropriate water vapor absorption lines are located.

TABLE ES1. Quantities derived from Raman Lidar System

Physical Quantity	Measurement Principle
Particle Backscatter	Measured at 355, 532 and 1064 nm with Klett algorithm implemented for the retrieval in the infrared, and calculated through a ratio of elastic and pure rotational Raman signals in ultraviolet and visible spectral range.
Particle Extinction	Derived directly from atmospheric attenuation of pure rotational Raman signals at 355 and 532 nm.
Depolarization Ratio	Measured at 532 nm as a ratio of two components of lidar backscatter signal having their vectors of the electromagnetic field oriented perpendicular and parallel with respect to those of the linearly polarized sounding laser beam.
Water Vapor Mixing Ratio	Derived as a ratio of ro-vibrational Raman signals due to water vapor and nitrogen molecules with excitation at 355 nm.
Air temperature	Measured at 355 nm with a pure rotational Raman lidar technique.

TABLE ES2. Uptime (% by Season) of main BCO instrumentation in first five years of operation. MRR refers to the Metek Micro Rain Radar, two of which are operational, one at the CIMH the other at the BCO.

Season	DJF	MAM	JJA	SON
Cloud Radar	59	38	55	46
Raman Lidar	77	55	42	69
MRR-BCO	94	98	90	94
MRR-CMHI	84	99	99	73
Ceilometer	91	94	90	94
CloudCamera	96	98	69	71
Weather	90	79	53	60

TABLE ES3. Overview of NARVAL South Phase Flights. OBF is the airport code for Oberpfaffenhofen in South Germany, BGI stands for Grantley Adams International Airport in Barbados. All times are UTC.

Mission	Date	Take-Off	A-Train	Landing	Comment
RF01	10.12.2013	1014 (OBF)	1507	2041 (BGI)	Trans Atlantic
RF02	11.12.2013	1429 (BGI)	1724	2158 (BGI)	Local flight
RF03	12.12.2013	1350 (BGI)	1629	2020 (BGI)	Mid Atlantic
RF04	14.12.2013	1335 (BGI)	1629	2021 (BGI)	Mid Atlantic
RF05	15.12.2013	1515 (BGI)	1700	2145 (BGI)	Mid Atlantic, Pitch and Roll Maneuvers
RF06	16.12.2013	1310 (BGI)	1605	2259 (OBF)	Trans Atlantic
RF07	10.12.2013	1005 (OBF)	n/a	1957 (BGI)	Trans Atlantic, coordinated operations with F20
RF08	10.12.2013	1620 (BGI)	1723	0235 (OBF)	Trans Atlantic

LIST OF FIGURES

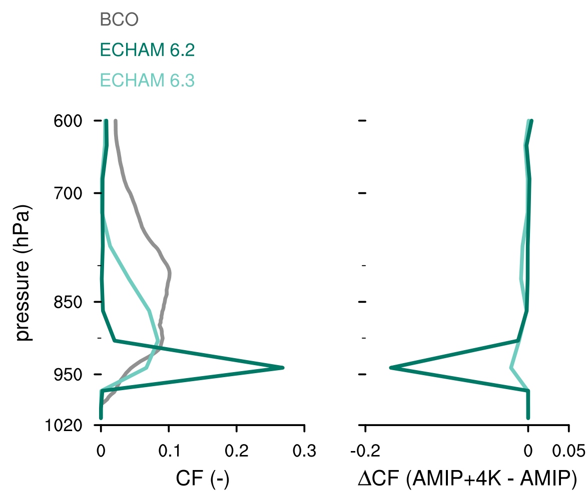

651 FIG. 1. Cloud fraction (left) and change in cloud fraction (right) for the ECHAM6 atmospheric general circulation model. Shown by the teal colored lines are two versions of the model that differ in the mixing parameter used in the parameterization of shallow convection. Cloud fraction derived from measurements (gray) at the Barbados Cloud Observatory are shown for reference in the panel on the left.

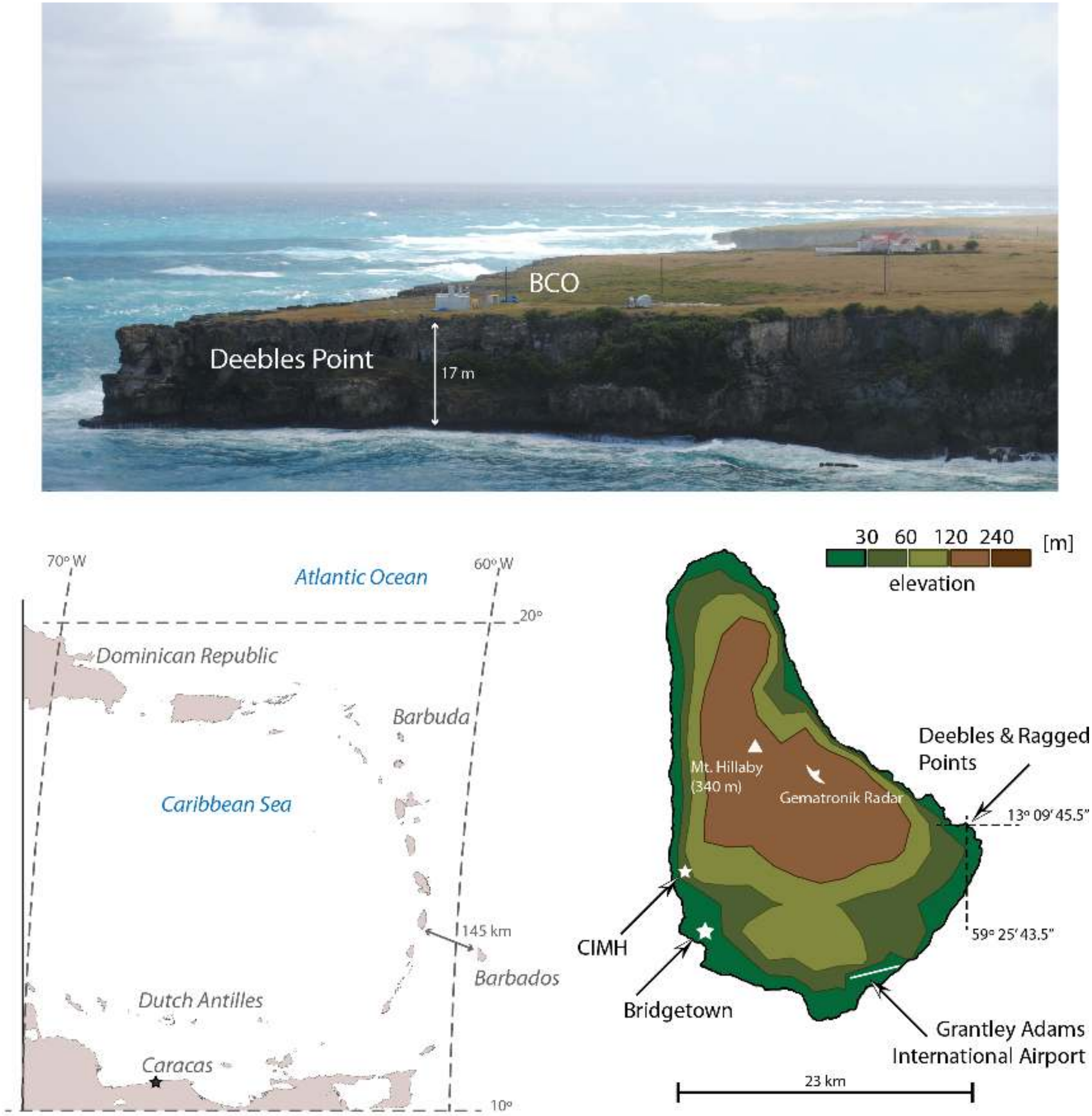

FIG. 2. Setting of Barbados Cloud Observatory: Photograph of the observatory as seen from neighboring Ragged Point (upper); Location of Barbados relative to other land masses that give definition to the Caribbean Sea (bottom left); Observational Infrastructure on Barbados and island relief as taken from the 1' ETOPO1 global relief model **?**.

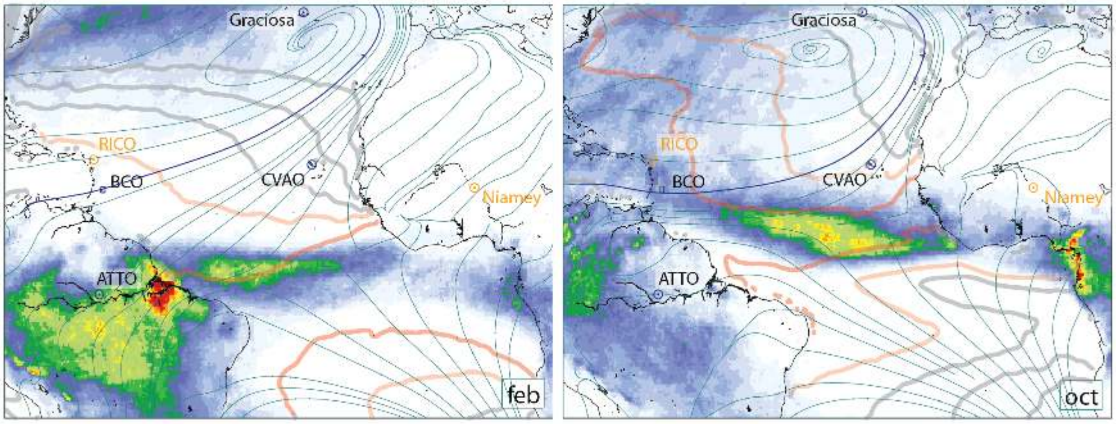

FIG. 3. Seasonal snapshots of tropical Atlantic and neighboring land masses for climatologically wettest (October) and driest (February) months on Barbados. Shown are shaded contours of TRMM precipitation (ranging from 1 to 16 mm d^{-1}), streamlines of near surface (10 m) winds from the ERA-Interim reanalysis, and sea-surface temperature monthly climatological mean (contour lines every 2 °C with orange lines denoting 26 °C and 28 °C isotherms) from AMSR-E measurements. Other BCO-like observatories are also indicated on the map, these include the permanent stations: Amazon Tall Tower Observatory (ATTO), the Cape Verde Atmospheric Observatory (CVAO), and the ARM facility on Graciosa, as well as locations of recent field measurements as part of RICO (Rain in Cumulus over the Ocean) which took place in 2004-2005, and the ARM mobile facility which was located in Niamey Niger through 2006 as part of the African Monsoon and Multidisciplinary Analyses Programme, AMMA.

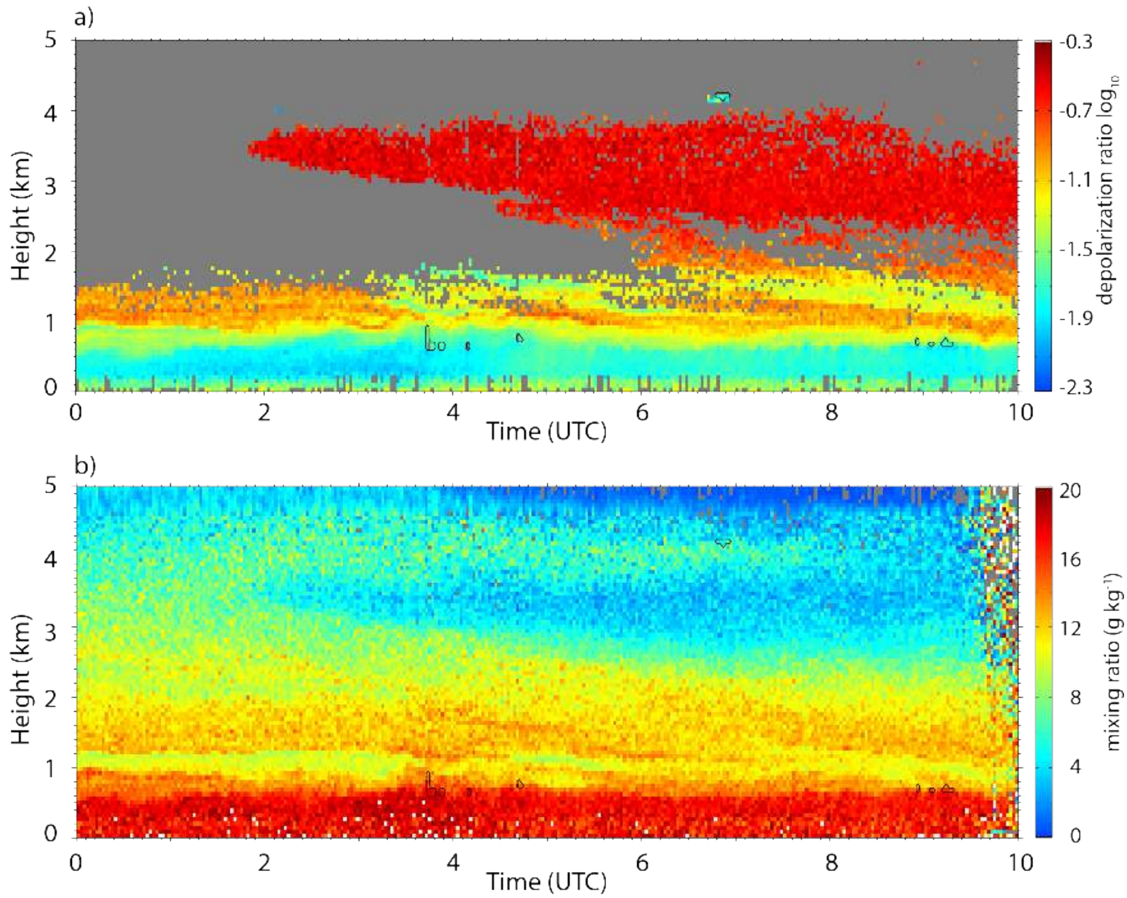

FIG. 4. Time series of Raman profiles showing a dust intrusion over the BCO on 10 August 2011. The Saharan dust layer is well visualized by a strong increase in the linear depolarization (panel a) in a layer near 3 km after 2 UTC. In panel b the humidity retrievals from the Raman lidar also show the dust layer is also a dry intrusion.

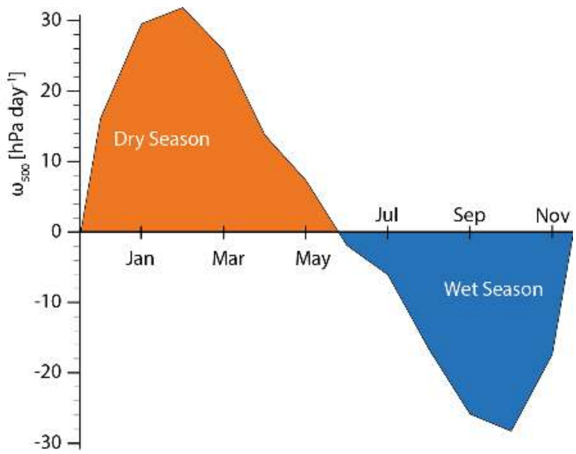

FIG. 5. Monthly climatology (seasonal cycle) of mid-tropospheric vertical pressure velocity (ω_{500}) over Barbados region (12-15N, 58-60W)) as represented in the ERA-Interim dataset (1989-2007).

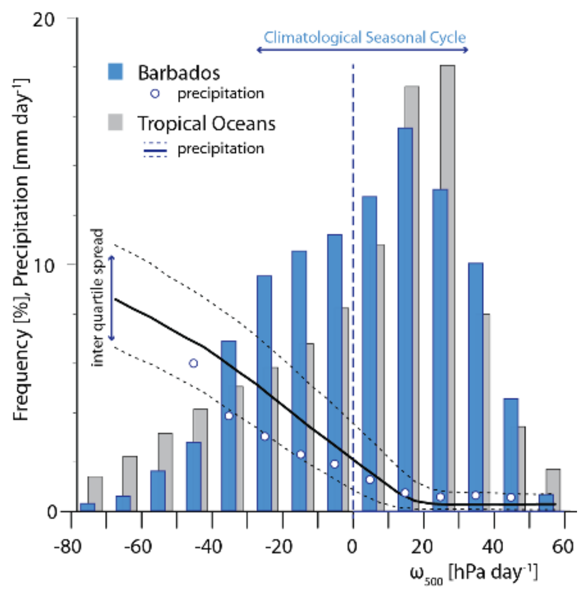

FIG. 6. Distribution of monthly averaged vertical pressure velocity from the ERA-Interim data overlain with precipitation conditioned on a given range of vertical pressure velocity for the entire maritime tropics (30°S-30°N) and over the Barbados region (12 °N - 15 °N, 58 °W-60 °W) as represented in the ERA-Interim dataset (1989-2007).

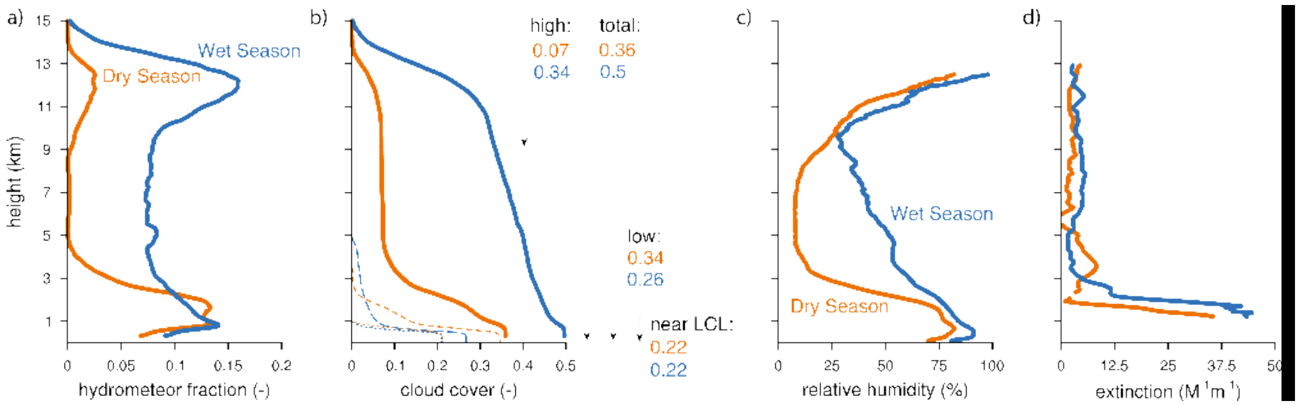

FIG. 7. Vertical profile of hydrometeor fraction (a) from radar; cumulative cloud cover (b), from radar (thick solid), ceilometer up to 5 km (thin-dashed) and up to 1 km (thin-dotted); relative humidity (c); and clear-sky extinction (d). Data in panels (c) and (d) are from the Raman lidar. Shown are results from October (wet season) and February (dry season)

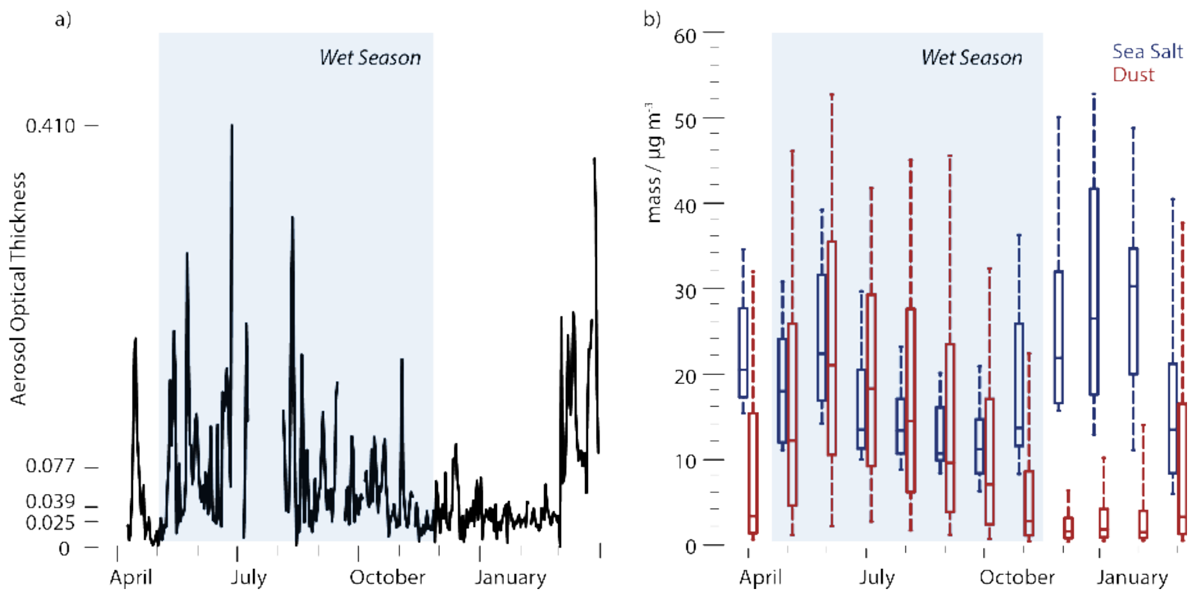

682 FIG. 8. (a) Time-series of Raman lidar optical depth at 335 nm integrated between 0.5 and 15 km during first year of BCO operations. Tick marks on *y*-axis denote minimum maximum, median and interquartile range of data. (b) Daily median, interquartile and 10-90% values of dust and sea-salt measured from ten years (2000-2010) of filter samples at Ragged Point.

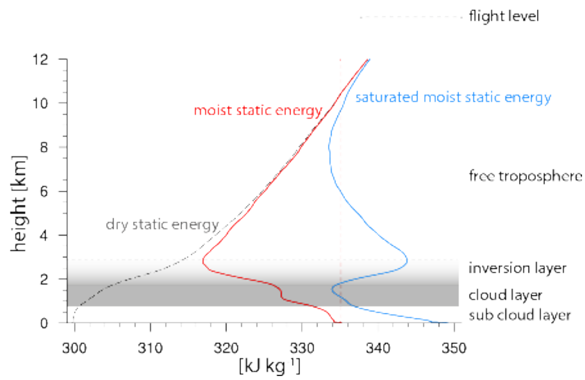

686 FIG. 9. Trade wind sounding from forty-six dropsondes launched during a ten day period over the north-central sub-tropical Atlantic. Dry static energy, s shown by black dashed line, moist static energy, h in red and saturation moist-static energy h_s in blue. The relative position of h between s and h_s measures the relative humidity.

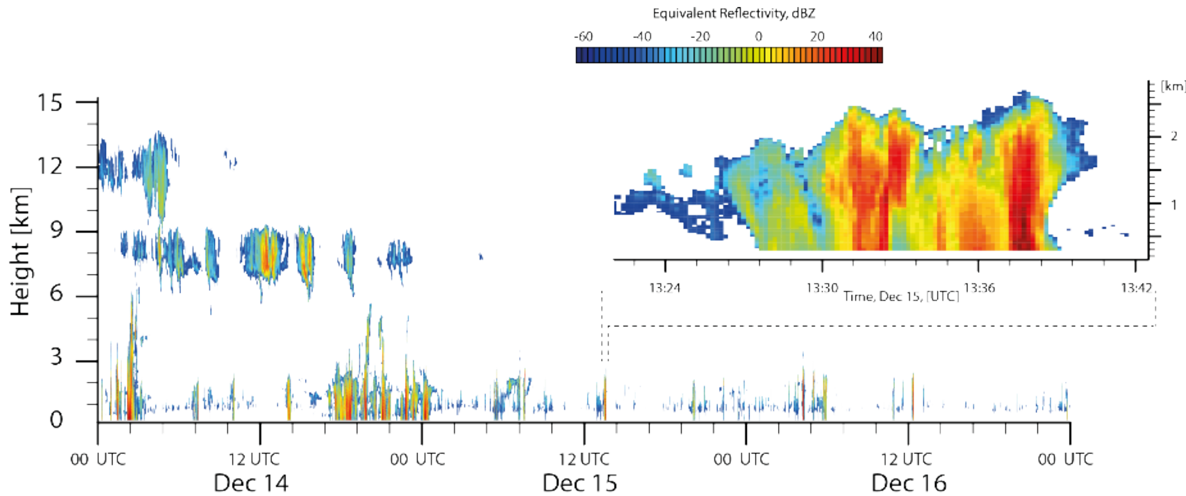

690 FIG. 10. Radar reflectivity profiles from the KATRIN cloud radar at the BCO for the three day period of 14-16 December 2014. Inset shows the details of a convective system passing over the site near 13:30 UTC on 15 December 2015 with a maximum echo larger than 40 dBZ near the surface at 1338 UTC arising from a systems whose echo tops were at an altitude of less than 3 km.

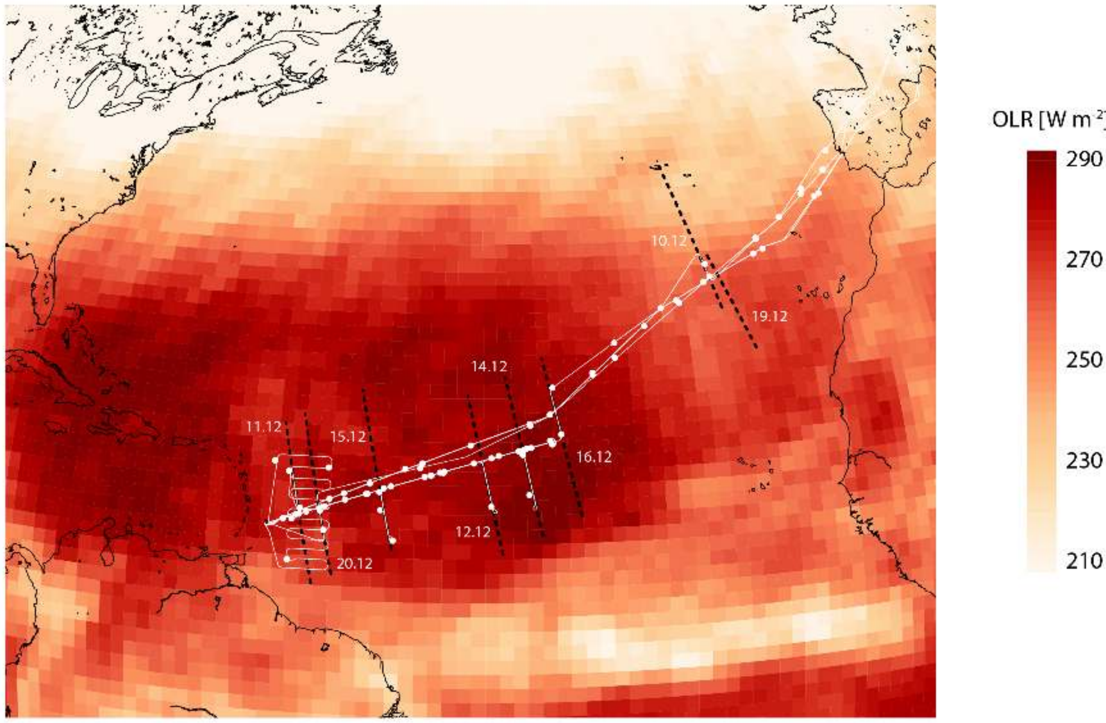

694 FIG. 11. Overview of HALO Trade-wind flights. Shown are the flight paths during the Southern NARVAL (Next Generation Aircraft Remote Sensing for Validation Studies) Campaign. Eight flights were performed, three of which departed from HALOs hope base of Oberpfaffenhofen south-east of Munich. Seven flights included A-train under flight legs (evident as NNE-SSW jigs) for intercomparisons with CloudSat and CALIPSO.

FIG. B1. HALO with the remote sensing bellypod mounted to its fuselage, left. Closeup image of belly pod showing three compartments for Cloud Radar, water vapor lidar and three bank, 26 channel radiometer.

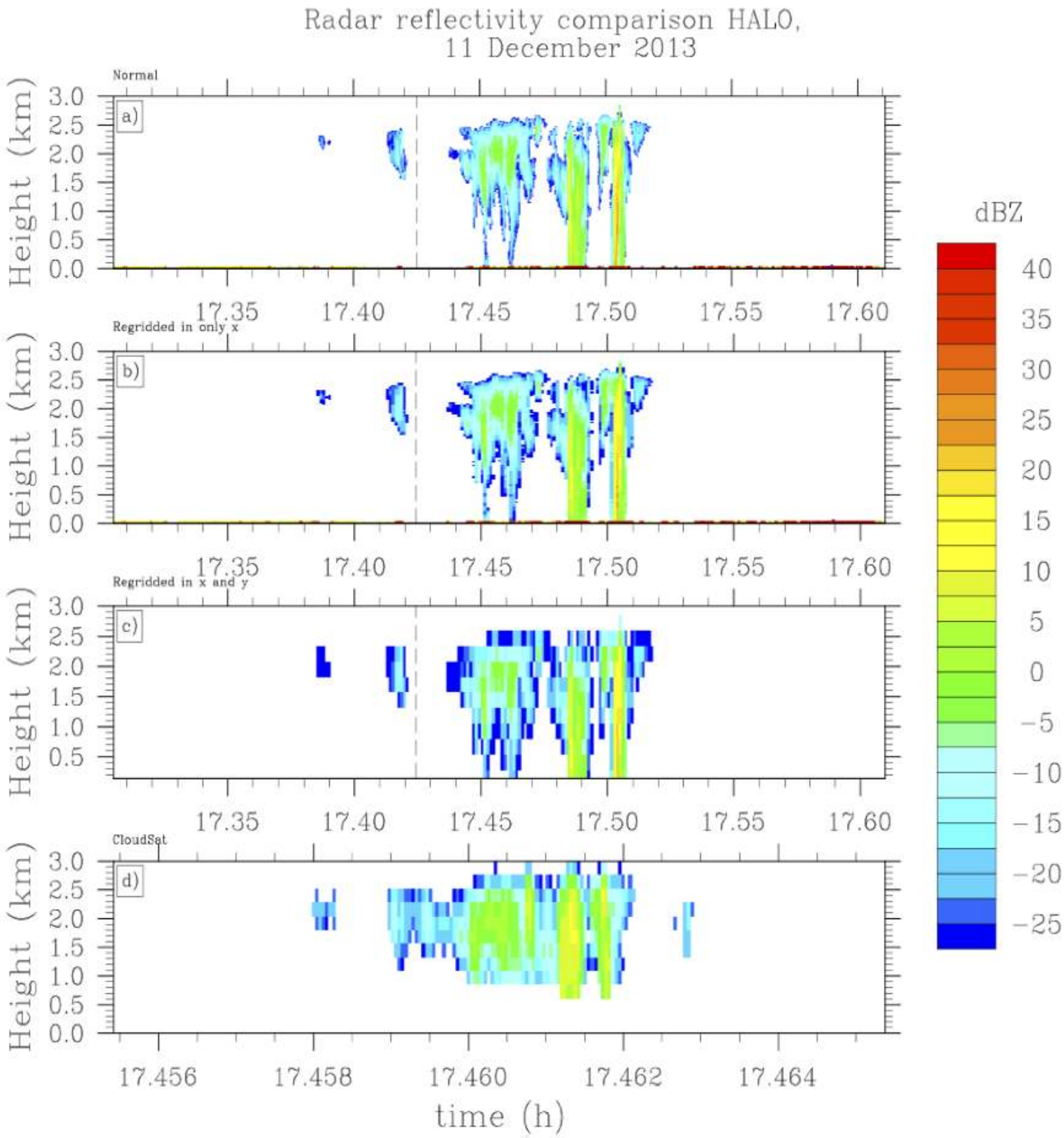

FIG. ES1. CloudSat overpass along a HALO leg on 11 Dec 2013. Shown is the K_α reflectivity from the HALO cloud radar (a); regretted to match the resolution of CloudSat in the horizontal (b); to match CloudSat horizontal resolution and vertical range gating (c); CloudSat data (d). The point of coincidence is indicated by the dashed line.